Freeze-dried matrices for ocular administration of bevacizumab: a comparison between subconjunctival and intravitreal administration in rabbits

Susi Burgalassi[a], Daniela Monti[a], Nadia Nicosia[a1], Silvia Tampucci[a], Eleonora Terreni[a], Andrea Vento[b], Patrizia Chetoni[a]

[a]Department of Pharmacy, University of Pisa, Pisa, Italy

[b]Ophthalmology Unit, Versilia Hospital, Azienda USL Toscana nord ovest, Viareggio, Italy

[1]Present address: Cosmofarma

Corresponding author:

Daniela Monti

Department of Pharmacy, Unive

via Bonanno 33, I-56126 Pisa, I

Phone: +39 050 2219662

E-mail: daniela.monti@unipi.it

ORCID: Susi Burgalassi	0000-0002-0795-2886
Daniela Monti	0000-0001-7622-4367
Nadia Nicosia	-
Silvia Tampucci	0000-0002-8927-6083
Eleonora Terreni	0000-0002-2280-4013
Andrea Vento	-
Patrizia Chetoni	0000-0003-4790-4683

Acknowledgements This work was funded by University of Pisa (grant PRA 2016_27). The authors would like to thank Dr Carla Lenzi and Prof Giancarlo De Montis for technical support to histological analysis and the relevant interpretation of the results.

Abstract

This work was aimed to tune solid matrices for bevacizumab (BVZ) subconjunctival or intravitreal administration in order to prolong drug release, to reduce the number of applications and consequently the side effects. Matrices, with sizes suitable for intravitreal or subconjunctival administration, based on hydroxypropylmethyl cellulose (HPMC), polyvinylpyrrolidone (PVP), polyvinyl alcohol (PVA), and polyacrylic acid (PAA) were obtained by freeze-drying of polymeric dispersions either in phosphate buffer solution or water and were sterilized by gamma rays. The matrices were characterized from the technological point of view and evaluated for in vitro release of Dextran and BVZ. In vivo evaluation of BVZ release in ocular humours was finally carried out on rabbits. The obtained matrices showed solvent sorption time ranging from a few seconds for PAA to 46 minutes for HPMC, with shorter times when prepared in buffer solution. The hydration times were up to 5.5-fold higher after sterilization. HPMC and PVA matrices showed a slowdown of the release rate of both Dextran and BVZ, but HPMC was selected for following in vivo studies also in consideration of its higher viscosity after rehydration of the matrix. HPMC matrix was well tolerated by the rabbit eye when intravitreally and subconjunctivally administered. The different treatment produced the same effect in terms of drug concentration in aqueous and vitreous humour up to 12 weeks after administration. The results of this study support the possible use of lyophilized matrices as a BVZ delivery system to the posterior segment of the eye.

Key words: bevacizumab, subconjunctival, intravitreal, rabbit, freeze-drying, matrices

Introduction

The diseases in the posterior segment of the eye are commonly diagnosed in ageing population. The most prevalent posterior eye diseases that causes visual impairment include age-related macular degeneration (AMD), macular oedema secondary to retinal vein occlusion and diabetic retinopathy (DME) and cystoid macular oedema [1]. AMD is the commonest cause of blindness in industrialized countries, 7% of all blindness (3 million persons). Visual loss from this condition is uncommon among persons under the age of 50, but the number affected is expected to increase as a result of the population ageing. At least 180 million people worldwide have diabetes and, as its complication, DME is responsible for 4% of the cases of blindness due to eye diseases [2].

To data, several drugs are known to improve the course of these pathologies and the most attractive and interesting but also difficult challenge facing by the pharmaceutical researcher is the drug delivery to posterior segment of the eye. Topical, systemic, intravitreal and periocular routes can be used to this purpose. The topical route, even if the most complying for patients, is subjected to loss due to rapid drainage and systemic absorption which, added to low permeability of the corneal epithelium, make this route inefficient in delivering therapeutic concentrations of drug to the back of the eye. Conversely, the blood-retinal barrier prevents the diffusion of systemically administered drugs towards the inside of the eye. Therefore, the most suitable routes of drug delivery to the posterior segment are the intravitreal and the periocular ones. Currently, the drug intravitreal administration to the retina is widely used, even if the frequent use of this route can lead to complications that include eye pain, inflammation, infection, visual disturbances, but also more severe adverse events. The need to repeat the administration, even at an early date, greatly increases the risk of side effects. The periocular routes are a good alternative since the sclera presents a larger surface area, a higher permeability and a lower protease activity in comparison with cornea. Subconjunctival administration enables the drug to bypass the conjunctiva–cornea barrier, giving direct access to the trans-scleral route. In spite of this, only small amounts of drug reach the vitreous body via trans-scleral route given the physiological loss factors [3].

At present, anti-VEGFs are at the forefront of treatment for various back of the eye diseases and drugs such as aflibercept, ranibizumab and bevacizumab are today largely used. Macromolecular drugs display numerous limitations related to delivery such as absorption/permeability across biological membranes, poor bioavailability and stability. Besides, their short in vivo half-life implies frequent administrations that lower patient compliance [4].

An approach to overcome the problem of rapid elimination of these molecules from the administration site could be the development of a solid dosage form able to provide prolonged drug release.

The aim of the present work was the development of matrices prepared by freeze-drying from polymeric dispersions for the delivery of bevacizumab to the posterior segment of the eye. Different polymers were employed to prepare the matrices that were subjected to technological characterization. The formulations with the highest hydration time and able to low the drug release were evaluated in vivo on rabbits.

Materials and methods

Materials

Polyacrylic acid, PAA (Carbopol® 980, BF Goodrich Co., Holland); Polyvinyl alcohol, PVA (PolyViol® 4-88, Merck, Germany); Hydroxypropylmethylcellulose, HPMC (Methocel® K4M Premium EP, Colorcon, Italy); Polyvinylpyrrolidone, PVP (Kollidon® 90F, Basf, Germany); Fluorescein isothiocyanate-dextran 150 kDa, FITC-DX (Sigma-Aldrich, Sweden); Bevacizumab, BVZ, commercial solution containing 25 mg/ml (Avastin®, Roche, Swiss), trehalose (SG, Hayashibara Co., Japan), mannitol and lactose (EUPh grade, Carlo Erba, Italy). All other chemicals were of reagent grade.

Methods

Polymeric vehicles under study

HPMC, PVP and PVA dispersions were obtained by slowly adding the polymers to pH 7.4 Sørensen phosphate buffer solution (PBS) or MilliQ water (Millipore) under stirring at room temperature, or heating for 1 h at 50 ˚C for PVA; PAA dispersions were obtained by adding the polymer to MilliQ water and partially neutralizing to pH 6.0 by 1N NaOH solution. Some formulations contained mannitol, as summarized in the Table 1, while the PAA dispersion was added with lactose. All formulations had 1.0% trehalose as cryo- and lyo-protectant.

Preparation of lyophilized matrices

Lyophilized matrices were prepared freeze-drying (VirTis Wizard 2.0) aliquots of the formulations under study: 1.0 g of dispersion into glass vials for water sorption time determination; 20.0 g into teflon dishes for rheological measurements; and 50.0 µl into cylindrical moulds of silicone for drug stability and release studies. For these latest studies, either FITC-DX, as model macromolecule, or BVZ were added to polymeric vehicle under stirring in the ratio 0.625 mg in 50.0 µl before freeze-drying.

Formulations were freeze-dried under the following controlled conditions:

1) Freezing: Pressure 400 Torr; Temperature -38 °C; Rate 0.6 °C/h; Extra freeze time 120 min.

2) Primary drying: Pressure 100 Torr; Temperature -38 to 0 °C; Rate 2.1 °C/h.

3) Secondary drying: Pressure 50 Torr; Temperature 0 to 25 °C; Rate 5.0 °C/h; Extra drying 27 °C for 60 min.

The matrices were then stored in desiccators until use.

Sterilization

Three batches of freeze-dried matrices, unloaded and loaded with FITC-DX or BVZ, were subjected to sterilization process with Cobalt-60 gamma ray technology (10 and 25 kGy, Gammatom srl).

Rheological measurements

Rheological measurements were performed at 25 °C on polymeric dispersions just prepared and after reconstitution to their original weight (20.0 g) by adding to the freeze-dried matrices the quantity of water removed during the process. The rheometer used was a Rheostress RS 1 (Haake) equipped with coaxial cylinders (Z40 and Z41) or cone and plate (C60/4-P61), at shear rates ranging from 0 to 200 s^{-1}. Some polymeric dispersions exhibited a pseudoplastic flow described by the Ostwald-de Waele power law: $\tau=KD^N$, and their apparent viscosity, η', was calculated for D = 1 s^{-1}.

Water sorption time

The time required to obtain a complete re-dispersion of matrices was determined and reported as Water Sorption Time (WST). WST was qualitatively monitored by digital microscope (Dino-lite Pro, ANMO, Taiwan): a lyophilized matrix was placed into a glass vial standing on graph paper; the quantity of water removed during freeze-drying process was added to the matrix to reconstitute it to original weight (1.0 g); the end-point was established when the lines of paper were again clearly visible.

Analytical methods

The fluorescence of FITC-DX in the matrices under study and in the experimental samples was measured at 520 nm (excitation 490 nm) by a fluorimeter (RF-551, Shimadzu) equipped with a LC-6A pump (Shimadzu), 20-µl Rheodyne injector and a computer integrating system. The mobile phase was Milli-Q water at a flow rate of 0.5 ml/min. The fluorescence was determined by comparison with a calibration curve built with FITC-DX increasing concentrations ranging from 0.55 (limit of quantification) to 8.22 µg/ml.

The amount of drug in the matrices and in the samples of the in vitro experiments (stability, release) was assayed by HPLC (LC-6A pumps, SCL-6B controller, SPD-10A detector and computer integrating system, Shimadzu Corp., and 20-µl Rheodyne injector). The column (Aeris widepore 150 x 4.6 mm, Phenomenex), equipped with a corresponding guard column, was packed with XB-C8 phase (size 3.6 µm) and thermostated at 70 °C. The mobile phase was acetonitrile + 0.1% trifluoroacetic acid (TFA) (phase A) and acetonitrile/water (8:92) + 0.1% TFA (phase B); the flow rate was 1.0 ml/min following a gradient elution: 76% B for 1 min; 60% B in 3 min; 11% B in 17 min; 11% B for 2 min. The determination was performed at 280 nm by comparison with a calibration curve built with BVZ increasing concentrations ranging from 0.083 (limit of quantification) to 0.500 mg/ml.

BVZ amount into samples from the stability studies (one matrix for batch) and from in vivo experiments was determined by ELISA test as described in previous papers [5-7]. Briefly, human recombinant VEGF

(variant 165) was used to capture BVZ and anti-human IgG horseradish peroxidase for its detection by tetramethyl benzidine added of hydrogen peroxide to develop the colour. Standard and biological samples were diluted with 0.1% BSA in PBS. A standard curve was built with BVZ increasing concentrations ranging from 0.0875 to 3.75 ng/ml at each repetition of assay. For each repetition a "blank" sample (BSA in PBS without BVZ) was also included.

Stability of bevacizumab

BVZ stability into the matrices after sterilization process was evaluated as drug concentration and hydrodynamic diameter of the macromolecules. The matrices were weighted to calculate the theoretical BVZ quantity, dispersed in appropriate volumes of MilliQ water and subjected to analysis by HPLC and ELISA methods. ELISA is a more expensive and longer to perform method of analysis than HPLC, so it was carried out only on a matrix for each of the three batches subjected to sterilization in order to confirm the drug content. From the concentration point of view, the high BVZ amount in the samples made HPLC a method reasonably appropriate for the determination.

Dynamic Light Scattering

Dynamic light scattering (DLS) measurements were conducted at 25 °C by Submicron Particle Size (N4 Plus, Coulter) equipped with a He-Ne laser (output power 10 mW at wavelength 632.8 nm) following the methodology described in Burgalassi et al. [8] to evaluate the presence of aggregates of drug molecules. BVZ commercial solution (50 μl) and HPMC-3 matrices, unloaded and loaded with BVZ, were dispersed in 3.0 ml of MilliQ water at room temperature. In order to eliminate the effect of dust particles, a 0.45 μm membrane was used to filter the samples and the diluent water into a dust-free cell before the measurements. Ten drops of the dispersion were added to diluent water contained in an appropriate cuvette. Two runs of triplicate measurements were made.

In vitro release study

Release in vitro of FITC-DX and BVZ from sterilized loaded matrices through cellulose ester dialysis membranes with MWCO 300 kDa (Spectrum Laboratories Inc., Holland) was investigated using Gummer-type vertical diffusion cells [9] with an available diffusion area of 1.33 cm^2. The donor phase consisted of a lyophilized matrix of 11.5 mm in length and 2.9 mm in diameter (Fig. 1) soaked with 10 μl of isotonic PBS; the receiving compartment contained 5.0 ml of isotonic PBS maintained at 37 °C and stirred at 600 rpm. The release system was sealed to avoid evaporation of donor phase and to protect it from light. At

predetermined intervals of time, 2 ml of receiving phase were withdrawn for analysis and replaced with the same volume of fresh fluid. Samples at low content of drug were concentrated 5:1 under vacuum (equipment RC 10.09/RCT 60, Jouan) before analysis. FITC-DX, as powder soaked with 10 μl of isotonic PBS, and BVZ commercial solution (25 μl) were used as controls. All experiments were performed three times.

In vivo studies on animals

The animals were used and treated as prescribed in the publication "Guide for the Care and Use of Laboratory Animals" (ILAR, 2011). All experiments conformed with the ARVO Statement for the Use of Animals in ophthalmic and Vision Research: they were conducted in compliance with protocols approved by the Organization responsible for Animal Welfare of the University of Pisa and Italian Ministry of Health (authorization n. 199/2016-PR).

Thirty-six male, New Zealand albino rabbits, three to four months old and weighing 3.0-3.5 Kg (Pampaloni Rabbitry, Italy) were housed singly in standard cages in a room with controlled lighting, at 19 ± 1°C and 50 ± 5% R.H., with no restriction of food or water. All animals were anesthetized by i.m. administration of 8.73 mg kg^{-1} tiletamine hydrochloride and 8.63 mg kg^{-1} zolazepam hydrochloride (Zoletil 100®, Laboratories Virdac, France).

The animals were divided randomly into two groups that received subconjunctivally or intravitreally (respectively SC and IVT group, n = 18) BVZ-medicated matrices in the right eye; the fellow eye was the control. Topical anaesthetic (oxybuprocaine hydrochloride, Novesina® 0.5%, Novartis Farma S.p.A., Italy) and disinfectant (povidone-iodine 5%, Betadine® topical solution diluted in phosphate buffer solution) eye drop were applied before surgical procedure then a blepharostat was inserted for holding the eyelids apart.

Matrices were introduced into a pocket created between sclera and conjunctive (SC), via a 4-5 mm incision in the superior quadrant at 7-8 mm from the limbus or in the vitreous humour (IVT) through a pars plana incision. The incisions were then closed with a central single suture.

Topical applications of a combination of tobramycin 3 mg/mL and dexamethasone 1 mg/mL (TobraDex®; S.A. Alcon, Belgium) were administered 3 times a day for 5 days after surgery.

Clinical evaluations were performed 2 hours after surgery until 2 weeks. Clinical examination included observation of inflammatory response via slit-lamp and indirect ophthalmoscopy, and IOP measurements. In detail, the eyes of the rabbits were daily observed, along the first week, for any change at the insertion

sites to evaluate any evidence of surgical complications, using slit-lamp examinations. At 7th day the eyes were examined using an indirect ophthalmoscope after dilation of pupil by tropicamide 0.5% (Visumidriatic®, Visufarma, Italy) to identify potential inflammation in the anterior and posterior segment. The IOP of both eyes of each rabbit was measured using a pneumotonometer (Digilab ModularOne, BioRad) under topical anaesthesia, every other day for two weeks, starting from the second postoperative day. Farther, treated eye of each animal was subjected to two digital photographic assessments in the week post-surgery, at 1st and 7th day.

The rabbits were euthanized by intravenous administration of an overdose of sodium pentobarbital solution (Pentothal sodium®, Gellini Farmaceutici, Italy) 2, 4 and 12 weeks after the surgical treatment; then the eyes were enucleated and aqueous and vitreous humours tested for BVZ amount using ELISA test. The retinas were isolated and underwent histology.

In order to reduce the number of animals used in the study, control groups (BVZ commercial solution by SC and IVT route) were not included in the experimental design and the discussion of the results was based on the data reported in the scientific literature.

Histological analysis

Retinal samples were fixed in 4% paraformaldehyde-phosphate buffer saline (0.1 M, pH 7.4), dehydrated and embedded in a plastic resin (JB-4 Embedding kit, Sigma-Aldrich, MO). Sections of 5 µm were cut by a microtome (Reichert-Jung), stained with methylene blue/toluidine blue, observed and photographed by a light microscope (Diaplan, Leitz).

Statistical analysis

Statistical differences between the means were assessed by Prism software v. 5.0f (GraphPad software Inc., S. Diego, CA). The evaluation included the mean of determinations and relevant standard error. Groups comparison was performed using the Student's two-tailed unpaired t-test; means were considered statistically different at $p < 0.05$ level.

Results and Discussion

The work was organized in two steps. The first one has been devoted to the preparation and technological characterization of polymeric vehicles without active substance. Such phase had the aim of choosing the

vehicle composition characterized by optimal technological and hydration properties. By the second phase, on medicated matrices, the stability and the *in vitro* and *in vivo* drug release was evaluated.

In Table 2, the viscosity values and the rheological behaviour of the polymeric dispersions before and after freeze-drying and sterilization processes are reported. PVP and PVA based formulations showed a Newtonian behaviour, while the other formulations showed a pseudoplastic behaviour. Observing the data reported into first column of the table, it can be noted that the viscosity of formulations can be variably influenced by the saline vehicle (formulations series 1). Salt presence does not affect viscosity of HPMC and PVA dispersions. The PBS vehicle weakly influences HPMCs viscosity, especially the K-type one, because of their higher total substitution: the viscosity values drop only at phosphate concentration exceeding 4 % [10]. The presence of salts into PVA dispersions initially leads to an increase of their apparent viscosity; a further increase of salt concentration causes a drop in values, as hydrogen bonding between solute and solvent is disrupted. However, also in this case, the salt concentration must be significant to appreciate the change [11], that is not our instance. On the contrary, the apparent viscosity of PVP dispersions decreased upon addition of salts [12], as in case of PBS: PVP-1 formulation in PBS vehicle, which shows a viscosity of 4.36 mPa s that rises to 24.42 mPa s when the water-dispersion is evaluated (PVP-2 formulation). The formulations based on PAA were prepared only in water, since it is known that polyacrylic acids change their molecular arrangement in presence of ions losing the typical gel structure.

After the freeze-drying process the viscosity values of Newtonian formulation remained the same while the viscosity values of pseudoplastic formulations decreased. Pseudoplastic behaviour is typical for asymmetric molecules that are extensively entangled and/or randomly oriented at rest. Under shear, these molecules become oriented and points of entanglement are reduced and consequently the resulting viscosity. The fall of viscosity values after freeze-drying can be attributed to phenomena of disentanglement of polymeric chains, actually freeze-drying of dilute solutions is an approach to achieve disentangled polymer samples [13].

The same behaviour was observed when the matrices were subjected to sterilization process by gamma rays: the viscosity values of Newtonian formulation remained the same while the viscosity values of pseudoplastic formulations decreased. Radiation normally affects polymers in two basic manners, both resulting from excitation or ionization of atoms. The two mechanisms are chain scission, a random rupturing of bonds, which reduces the molecular weight (i.e., strength) of the polymer, and cross-linking of polymer molecules, which results in the formation of large three-dimensional molecular networks.

In particular, in the case of HPMC-based formulation, not only the viscosity values decreased but the rheological behaviour changed: before the sterilization they showed a pseudoplastic behaviour with an apparent viscosity ranging between 379 and 411 mPa s, whereas after the sterilization the flux becomes Newtonian with viscosity values of about 43 mPa s. This phenomenon has been attributed to a change from a disperse structure to a globular form as a result of the influence of polymer chain rupture (depolymerisation), irrespective of the type of HPMC but related to the irradiation dose. Anyway, gamma rays have already been considered as a method for decontaminating HPMC raw materials or sterilizing HPMC-based pharmaceutical dosage forms [14].

As regard PAA formulations, 0.3% concentration (PAA-2/0.3) produced lyophilized matrices too much rigid and as a consequence too brittle. This brittleness made them difficult to handle without breakage, so it was not further investigated. Decrease in PAA concentration and increase in concentration of materials rapidly water-soluble (5.0% mannitol and 2.0% lactose) led to less rigid and brittle matrices.

To obtain an estimation of the rehydration time of the matrices when applied in vivo, WST was determined. WST of the lyophilized matrices before and after the sterilization process is reported in Table 3. In principle, the formulations prepared in PBS (formulations series 1) showed shorter WSTs than those prepared in water and a difference between WST values before and after the sterilization process was observed: WST values ranged from 3.1 to 5.5-fold higher with respect to the same matrices before the sterilization. The matrices PAA-based showed an extremely short WST, surely due to high percentage of hydrophilic material in the formulations. In fact, data summarized in the table highlighted that the matrices containing mannitol (formulations series 2) had shorter WSTs with respect to those without mannitol (formulations series 3). In these two series of formulations, the ability of hydration of the matrices did not vary much after treatment with gamma rays. Finally, based on the previous considerations, the matrices of the series 3 were selected for subsequent release studies, as presenting longer rehydration rates excluding PAA matrices.

Clearly, we have no certainty that rehydration times after in vivo administration are comparable in length to those observed in WST experiment, first of all due to the different composition of the biological fluid in which the matrix will have to be hydrated. Moreover, the use of simulating fluids, for example, the vitreous humour, is rather complicated given the nature and characteristics of the fluid itself [15]. However, the determination of WST values is a relative measure useful for evaluating the behaviour of one matrix against the other. The use of WST parameter as discriminating for the choice takes in account this criterion.

At the first, FITC-DX with a molecular weight of 150 kDa, the same of BVZ, was used as model molecule for the release studies from the matrices under investigation in order to choose the best polymeric matrix for BVZ delivery.

Figure 2 shows the cumulative amount of FITC-DX released from the loaded matrices. PVP-3 matrix was not able to control release of FITC-DX, in fact its release profile was similar to that of FITC-DX used as control, whereas HPMC-3 and PVA-3 matrices showed release rates lower than control. After 7 h, PVP-3 matrix released a percentage of FITC-DX of 21.52±3.27%, followed by PVA-3 matrix (4.92±1.35%), and HPMC-3 matrix (2.62±0.97%). From these results it could be stated that the release of macromolecules of dextran type used here does not depend only on WST of the polymeric matrices and then of the polymer solubility. Other parameters appear to play an important role in determining the release rate such as the viscosity of the formulation after rehydration: in fact, HPMC-3 is the matrix which has a much higher viscosity with respect to the other two after hydration (46.12 versus 17.68 and 2.93 mPa s respectively for HPMC-3, PVP-3 and PVA-3) and, as a consequence, leads to a slowing of the release rate. In addition, the ability of the different polymers to form hydrogen bonds can become significant: HPMC and PVA are molecules highly hydroxylated which show a strong tendency to form inter- and intra-chain hydrogen bonds [11,16,17] also with FITC-DX by determining a slowing of its release from the hydrated matrix.

After preliminary studies, PVP-3 matrix was excluded from the following release experiments and only HPMC-3 and PVA-3 matrices were submitted to in vitro BVZ release studies; a BVZ solution was used as control. The results are reported in Figure 3. Both matrices seemed able to slow the release of the macromolecular drug, even if HPMC-3 to a statistically greater extent ($p=0.045$, unpaired t-test): after 96 hours, the amount of drug released from HPMC-3 matrix was 1.855±0.099% with respect to 3.533±0.074% of PVA-3. Then, both the matrices may be considered for prolonged release of BVZ but HPMC-3 was selected for following in vivo studies not only for its longer rehydration time but also in consideration of its higher viscosity after rehydration, which should lead to a longer residence time of the matrix in the ocular tissues and fluids.

The results of the stability studies showed a BVZ mean content into PVP-3 and HPMC-3 matrices determined by HPLC of 648.1±115.6 and 601.0±89.1 μg, corresponding to 103.7±18.5 and 96.2±14.3 % w/w of the theoretical amount, respectively for low (10 kGy) and high (25 kGy) ray dose exposition, irrespective of the type of polymer used in the formulation. The results obtained by ELISA test for HPMC-3 matrix confirmed these data as a BVZ mean content of 598.8±34.5 (95.8±5.5 % w/w) and 647.6±32.9 μg (103.6±5.3 % w/w) after low and high ray dose was found. The statistical comparison by unpaired t-

test of the four groups of analysis never resulted in significant differences (p values between 0.364 and 0.997).

The results obtained from the analysis by DLS showed a hydrodynamic diameter of bevacizumab commercial solution of 24.28±2.92 nm, attributed to both BVZ monomer and dimer form. A unique population was also revealed when HPMC-3 matrix was analysed, with size of 83.68±4.36 nm: the size was consistent with what was found by Burgalassi et al. [8]. DLS analysis of the BVZ-loaded HPMC-3 matrix showed the appearance of two other population peaks around 70-90 and 600-700 nm in addition to that due to the monomer and dimer form of the drug. The population peak of 70-90 nm was attributed to the polymer while that of 600-700 nm could be assigned to BVZ in an aggregated form. BVZ aggregated form was represented in a small extent, about 5% when expressed in volume intensity: more precisely 5.78 and 5.52%, respectively for dispersions derived from matrices irradiated with 10 and 25 kGy. These results are in line with the data previously reported by Paul et al. [18] in a study on Avastin® repackaged in syringes. The hydrodynamic diameter sizes obtained in this study supported the drug stability in terms of protein aggregation.

From these results here we can state that lyophilisation is a suitable technique to obtain a solid dosage form of bevacizumab as highlighted also by other authors [19-22]. A key point for maintaining the stability of the protein drug is the presence in the formulation of the trehalose acting as cryoprotectant [23]. Even the sterilization process, though considered critical for this type of molecule, does not seem to have a very negative impact on BVZ stability. This is probably due to the fact that the irradiation is carried out on a dry product, and not in water solution. In fact, it is known that free radicals and reactive oxygen species derived from water irradiation are the most responsible for damage that occurs in protein samples after conventional gamma sterilization processes [24,25]. Moreover, this study showed no significant differences in the content of drug among the matrices irradiated with 10 or 25 kGy making possible to apply the highest dosage of gamma rays for greater process safety. In any case, in this study we did not take care to investigate the effective sterility of the matrices. This could indirectly be inferred from the fact that during in vivo experiments there were no cases of infection.

The formulation selected (HPMC-3 loaded with 0.625 mg of BVZ) was surgically administered in the eyes of albino rabbits. The concentrations of BVZ in the aqueous and vitreous humours after subconjunctival (SC) or intravitreal (IVT) HPMC-3 administration are shown in Figure 4. The drug concentration was basically higher in the vitreous humour than in the aqueous humour at the shorter times after administration (2 and 4 weeks) and the statistical evaluation highlighted significant differences only

between BVZ aqueous and vitreous concentrations for the same treatment type. The different treatments seemed to produce the same effects as drug concentration into the ocular humours. On the contrary, at 12 weeks the data were very similar ranging from 2.93±0.24 to 4.72±0.68 ng/ml but at this time statistically significant differences (p=0.0178, unpaired t-test) between BVZ concentrations in vitreous humour after SC and IVT treatment were observed. BVZ concentrations into the rabbit ocular humours at 2 weeks observed in our study were lower than those reported for intravitreal injection of 50 μl commercial solution (1.25 mg BVZ, Avastin®), although these have a high variability ranging from about 3 to 100 and from 0.3 to 10 μg/ml for vitreous and aqueous humours, respectively [5-7, 26-31], not justified by the two-fold higher dose administered. Anyway, to our knowledge, only one study monitored the drug amount in the ocular humours for at least 12 weeks, and at this time the concentrations derived from standard commercial solution were not detectable [28]. Instead, for what concern subconjunctival administration, this study noticed higher BVZ concentrations in aqueous and vitreous humours with respect to those determined after SC administration of 50 or 100 μl Avastin® (1.25 or 2.50 mg BVZ) [29,32]. Several studies have described a number of BVZ delivery systems to posterior segment of the eye administrable by topical, subconjunctival and intravitreal route, as such liposomes [26,33], nano- and micro-vehicles [19,20,27,31,34,35], also SLN [36], and thermosensitive hydrogels [7,28,37], even if a few have not been in vivo tested. By analysing the results of the studies already published in comparison with those obtained in this work, it can be noticed that the drug concentrations assured by HPMC-3 lyophilized matrices are not the highest. However, the different routes of administration, the different experimental designs and especially the different duration of in vivo experiments make the results very difficult to compare. Definitely, higher intraocular drug concentrations, in the order of 15 and 1.2 μg/ml in vitreous and aqueous humour, respectively, were found 42 days after IVT administration in rabbits of 1.25 mg BVZ encapsulated in liposomes [26] or microspheres [31]. Even the intravitreal administration of 6-7 μg BVZ in nanoparticles resulted in BVZ concentration of about 10 μg/g (10 ng/mg) in the rat vitreous humour [22]. However, many authors have had similar results to those obtained by us especially using hydrogels. Rauck et al. [7] developed a urethane-based thermoresponsive biodegradable hydrogel, which produced high BVZ concentrations in aqueous humour at short time after administration but lower concentrations at long time with respect to those found after administration of HPMC-3 despite the administration of a two-fold higher BVZ dose. At 63 days, BVZ concentration was already lower than that determined in our study at 12 weeks after IVT administration, 2.93±0.24 ng/ml. Unfortunately, these authors did not analyse BVZ presence in vitreous humour. Instead, the same our BVZ concentrations into the vitreous were found by

Xie et al. [37] 4 weeks after IVT injection in rats of a different thermosensitive hydrogel based on PLGA-PEG-PLGA polymer and containing 0.3 mg of BVZ. Silk fibroin has also been used as a vehicle for 1.25 mg BVZ-loaded hydrogel. Its IVT injection in rabbits produced BVZ concentrations of 1.2±1.8 and 0.08±0.14 μg/ml, respectively in vitreous and aqueous humours, 90 days after the administration demonstrating a sustained release [28]. These amounts were much higher than ours but it is important to emphasize the extreme variability of published data, as demonstrated from standard deviation values.

While there are many publications that report intravitreal administration, little experimentation has been made on the possibility to reach the posterior segment by BVZ administering through other routes. Davis et al. [33] topically administered 0.75 mg of BVZ in annexin A5-associated liposomes leading to BVZ concentration of about 3 ng/g into rabbit vitreous after 5 days of treatment nothing compared to the concentrations found (about 1.5 μg/ml) in posterior segment 30 minutes after a single cell-penetrating peptides 0.5 mg BVZ eye drop application by de Cogan et al. [38].

In our experiments, the BVZ lyophilized matrices produced similar concentration into ocular humours when both intravitreal and subconjunctival way was used for administration. This is not surprising since the sclera is known to be permeable even to protein macromolecules as monoclonal antibodies given its structure consisting of a fibre matrix through which the drugs are able to diffuse [39,40]. It is supposable that the hydration time of the matrix and the subsequent onset of drug delivery from it may be slower after subconjunctival administration, due to the low presence of liquid in this space compared to the ocular posterior segment. This phenomenon is not apparent in our results as it happens in a shorter time than our first sampling so what we observed is the diffusion through the sclera already in the steady-state. The half-life ($t_{1/2}$, calculated by PKSolver in Microsoft Excel) values in the vitreous humour were 2.27 and 2.22 weeks after SC and IVT administration, respectively, similar to that presented by Lovett et al. [28] after IVT injection of 1.25 mf of BVZ in a hydrogel and longer than those reported by other authors. It is noteworthy that there is a significant difference in vitreous concentrations at 12 weeks between the two treatment types, probably due to the loss of a part of BVZ from subconjunctival matrices. In fact, it is known that drugs inserted into the subconjunctival space are cleared via trans-scleral or conjunctival blood and lymphatic flow, so a reduction of BVZ available to permeate across the sclera is justified [41].

In any case, after partitioning to some extent to the surrounding tissues, the drug can be eliminated from the vitreous through aqueous humour turnover and blood-ocular barriers. Although Bakri et al. [5] have described a pharmacokinetic model which resulted a very high distribution of BVZ from the vitreous into serum, Del Amo and Urtti [42] have used their own data showing that the BVZ elimination takes only via

anterior route. This behaviour produces similar pharmacokinetic profiles in aqueous humour from different administration routes as they are derived from similar vitreous concentrations, while the BVZ concentrations in aqueous lower than in vitreous are mainly due to the restricted access of the drug from vitreous to the aqueous.

Rabbits are widely used to study the ocular pharmacokinetics of drugs even if their use is often criticized as there are differences in the size of ocular cavities with respect to human eye. However, in a recent review on intravitreal pharmacokinetics in the rabbit and human eyes, Del Amo and Urtti [42] conclude that "*the rabbit is clinically predictable animal model for intravitreal pharmacokinetics, since both intravitreal volume of distribution and clearance values differ only moderately between rabbit and human*".

All of treated eyes displayed slight redness at the point of surgery that tended to disappear in the first week after treatment. In any case, no external signs of eye inflammation such as conjunctival or iridail redness, blinking, tearing and mucous secretion were observed. As an example, images at 1st and 7th day post-surgery are reported (Fig. 5). Indirect ophthalmoscopic observation did not display any sign of alterations of the inner chambers or the presence of the matrix, indicating that it completely rehydrates within a week. The gel derived from rehydrated matrix was never distinguishable from vitreous humour, at least to the naked eye, in the euthanized animals even after only 14 days. For the matter, the HPMC gel is colourless and its consistency is similar to that of the vitreous humour, so its presence is very hard to detect.

IOP values measured in the treated eye during clinical observation were reported as difference from the value measured in the fellow eye (ΔIOP) and are illustrated in Figure 6. Despite the high variability of the measures, the surgical technique does not appear to affect the intraocular pressure value.

The Figure 7 illustrates images by histological analysis comparing the retinal structure of untreated and treated eyes. No signs of alteration were detected in the retina of the intravitreally treated rabbits. The images show that the retinal layers were intact, with no evidence of inflammatory cell infiltration or morphological changes supporting the ophthalmoscopic observation.

Conclusions

Several studies have described ocular BVZ pharmacokinetics after topical, subconjunctival and intravitreal administration of different formulations, from the simple aqueous solution to hydrogel and nano-vehicles. Topical ocular dosage forms are the easiest to administer and the most accepted by patients but, although there is an extensive research of topically active formulations for BVZ delivery to

the posterior segment of the eye, the results so far obtained highlight the need for further work before these become a reality. However, no research compares different routes of administration of a likely drug delivery system and the intravitreal administration remains the beaten track.

The results of this study support the possible use of freeze-dried matrices as a BVZ delivery system to the posterior segment of the eye. Subconjunctival administration is certainly less invasive than the intravitreal one and appears to be able to sustain the drug release for an extended period of time, even though intravitreal practice could lead to more prolonged activity of the delivery system.

After considering the pharmacokinetic profiles, we proposed the use of subconjunctivally administrated lyophilized matrices as a new bevacizumab delivery system. The main advantages of a solid dosage form with respect to liquid formulations are both the stability, and therefore the preservation of the product, and the elimination of the possibility of drug loss by reflux from injection site.

This research opens new prospects for drug intraocular administration giving the basis on which to work for optimizing the formulation from technological and biopharmaceutical points of view. The formulation could be set up to provide higher drug concentrations for a longer period of time and also its consistency and design could be improved in order to facilitate the administration, perhaps with the aid of an injector.

All institutional and national guidelines for the care and use of laboratory animals were followed.

Conflict of interest The authors declare that they have no conflict of interest.

References

1. Agarwal A, Rhoades WR, Hanout M, Soliman MK, Sarwar S, Sadiq MA, Sepah YJ, Do DV, Nguyen QD. Management of neovascular age-related macular degeneration: current state-of-the-art care for optimizing visual outcomes and therapies in development. Clin Ophthalmol. 2015; https://doi.org/10.2147/OPTH.S74959

2. World Health Organization. Action plan for the prevention of avoidable blindness and visual impairment 2009-2013. WHO Document Production Services, Geneva; 2010.

3. Thrimawithana TR, Young S, Bunt CR, Green C, Alany RG. Drug delivery to the posterior segment of the eye. Drug Discov Today. 2011; https://doi.org/ 10.1016/j.drudis.2010.12.004

4. Joseph M, Trinh HM, Cholkar K, Pal D, Mitra AK. Recent perspectives on the delivery of biologics to back of the eye. Expert Opin Drug Deliv. 2016; https://doi.org/10.1080/17425247.2016.1227783

5. Bakri SJ, Snyder MR, Reid JM, Pulido JS & Singh RJ. Pharmacokinetics of intravitreal bevacizumab (Avastin). Ophthalmology. 2007; https://doi.org/10.1016/j.ophtha.2007.01.017

6. Ahn J, Kim H, Woo SJ, Park JH, Park S, Hwang DJ, Park KH. Pharmacokinetics of intravitreally injected bevacizumab in vitrectomized eyes. J Ocular Pharmacol Ther. 2013; https://doi.org/10.1089/jop.2013.0009

7. Rauck BM, Friberg TR, Mendez CAM, Park D, Shah V, Bilonick RA, Wang Y. Biocompatible reverse thermal gel sustains the release of intravitreal bevacizumab in vivo. Inv Ophthalmol Vis Sci. 2014; https://doi.org/10.1167/iovs.13-13120

8. Burgalassi S, Monti D, Tampucci S, Chetoni P. In vitro evaluation of some parameters involved in mucoadhesion of aqueous polymeric dispersions. Pharm Dev Technol. 2015; https://doi.org/10.3109/10837450.2014.943406

9. Gummer CL, Hinz RS, Maibach HI. The skin penetration cell: A design update. Int J Pharm. 1987; https://doi.org/10.1016/0378-5173(87)90053-6

10. Dow Brochure, ID 1051. Dow Chemical Company; 2015.

11. Briscoe B, Luckham S, Zhu S. The effects of hydrogen bonding upon the viscosity of aqueous poly(vinyl alcohol) solutions. Polymer. 2000; https://doi.org/10.1016/S0032-3861(99)00550-9

12. Güner A. Properties of aqueous salt solutions of polyvinylpyrrolidone. I. Viscosity characteristics. J Appl Polym Sci. 1996;62**:**785-8.

13. Teng C, Gao Y, Wang X, Jiang W, Zhang C, Wang R, Zhou D, Xue G. Reentanglement kinetics of freeze-dried polymers above the glass transition temperature. Macromolecules. 2012; https://doi.org/10.1021/ma300885w

14. Sebert P, Andrianoff N, Rollet M. Effect of gamma irradiation on hydroxypropylmethylcellulose powders: Consequences on physical, rheological and pharmacotechnical properties. Int J Pharm. 1993; https://doi.org/10.1016/0378-5173(93)90320-F

15. Su X, Tan MJ, Li Z, Wong M, Rajamani L, Lingam G, Loh XJ. Recent progress in using biomaterials as vitreous substitutes. Biomacromolecules 2015; https://doi.org/ 10.1021/acs.biomac.5b01091

16. Li H, Zhang W, Xu W, Zhang X. Hydrogen bonding governs the elastic properties of poly(vinyl alcohol) in water: Single-molecule force spectroscopic studies of PVA by AFM. Macromolecules 2000; https://doi.org/10.1021/ma990878e

17. Sahoo CK, Rao SRM, Sudhaka M. HPMC a biomedical polymer in pharmaceutical dosage forms. J Chem Pharm Sci. 2015;8;875-881

18. Paul M, Vieillard V, Roumi E, Cauvin A, Despiau MC, Laurent M, Astier A. Long-term stability of bevacizumab repackaged in 1 mL polypropylene syringes for intravitreal administration. Ann Pharm Fr. 2012; https://doi.org/10.1016/j.pharma.2012.03.006

19. Sharma G, Khalili A, Awwad S, Malik K, Matejtschuk P, Gaisford S, Brocchini S, Khaw P. Freeze drying to develop a bevacizumab-based tablet for ocular implantation. Invest Ophthalmol Vis Sci. 2013; 54: Abstract 1082.

20. Sousa F, Cruz A, Fonte P, Mendes Pinto I, Neves-Petersen MT, Sarmento B. (2017): A new paradigm for antiangiogenic therapy through controlled release of bevacizumab from PLGA nanoparticles. Scientific Reports. 2017; https://doi.org/10.1038/s41598-017-03959-4

21. Taniwaki L, Mendonça R, Cunha-Júnior AS, Faraco AAG, Ribeiro JAS, Scott IU, Jorge R. Effect of lyophilization on the in vitro biological activity of bevacizumab. Eye. 2010; https://doi.org/10.1038/eye.2010.96

22. Yandrapu SK, Upadhyay AK, Petrash JM, Kompella UB. Nanoparticles in porous microparticles prepared by supercritical infusion and pressure quench technology for sustained delivery of bevacizumab. Mol Pharmaceutics. 2013; https://doi.org/10.1021/mp400487f

23. Cleland JL, Lam X, Kendrick B, Yang J, Yang TH, Overcashier D, Brooks D, Hsu C, Carpenter JF. A specific molar ratio of stabilizer to protein is required for storage stability of a lyophilized monoclonal antibody. J Pharm Sci. 2001; https://doi.org/10.1002/1520-6017(200103)90:3<310::AID-JPS6>3.0.CO;2-R

24. Grieb T, Forng RY, Brown R, Owolabi T, Maddox E, McBain A, Drohan WN, Mann DM, Burgess WH. Effective use of gamma Irradiation for pathogen inactivation of monoclonal antibody preparations. Biologicals. 2002; https://doi.org/10.1006/biol.2002.0330

25. Silindir M, Ozer AY. Sterilization methods and the comparison of E-beam sterilization with gamma radiation sterilization. FABAD J Pharm Sci. 2009;34:43-53.

26. Abrishami M, Ganavati SZ, Soroush D, Rouhbakhsh M, Jaafari MR, Malaekeh-Nikouei B. Preparation, characterization, and in vivo evaluation of nanoliposomes-encapsulated bevacizumab (Avastin) for intravitreal administration. Retina. 2009; https://doi.org/10.1097/IAE.0b013e3181a2f42a

27. Andrew JS, Anglin EJ, Wu EC, Chen MY, Cheng L, Freeman WR, Sailor MJ. Sustained release of a monoclonal antibody from electrochemically prepared mesoporous silicon oxide. Adv Funct Mater. 2010; https://doi.org/10.1002/adfm.201000907

28. Lovett ML, Wang X, Yucel T, York L, Keirstead M, Haggerty L, Kaplan DL. Silk hydrogel for sustained ocular delivery of anti-vascular endothelial growth factor (anti-VEGF) therapeutics. Eur J Pharm Biopharm. 2015; https://doi.org/10.1016/j.ejpb.2014.12.029

29. Nomoto H, Shiraga F, Kuno N, Kimura E, Fujii S, Shinomiya K, Nugent AK, Hirooka K, Baba T. Pharmacokinetics of bevacizumab after topical, subconjunctival, and intravitreal administration in rabbits. Invest. ophthalmol. Vis Sci. 2009; https://doi.org/10.1167/iovs.08-3148

30. Sinapis CI, Routsias JG, Sinapis AI, Sinapis DI, Agrogiannis GD, Pantopoulou A, Theocharis SE, Baltatzis S, Patsouris E, Perrea D. Pharmacokinetics of intravitreal bevacizumab (Avastin®) in rabbits. Clinical Ophthalmol. 2011; https://doi.org/10.2147/OPTH.S19555

31. Ye Z, Ji YL, Ma X, Wen JG, Wei W, Huang SM. Pharmacokinetics and distributions of bevacizumab by intravitreal injection of bevacizumab-PLGA microspheres in rabbits. Int J Ophthalmol. 2015; https://doi.org/10.3980/j.issn.2222-3959.2015.04.02

32. Kim MJ, Han ES, Kim JW, Kim TW. Aqueous humor concentration of bevacizumab after subconjunctival injection in rabbit. J Ocular Pharmacol Ther. 2010; https://doi.org/10.1089/jop.2009.0022

33. Davis B, Normando EM, Guo L, Turner LA, Nizari S, O'Shea P, Moss SE, Somavarapu S, Cordeiro MF. Topical delivery of Avastin to the posterior segment of the eye in vivo using annexin A5-associated liposomes. Small. 2014; https://doi.org/10.1002/smll.201303433

34. Li F, Hurley B, Liu Y, Leonard B, Griffith M. Controlled release of bevacizumab through nanospheres for extended treatment of age-related macular degeneration. Open Ophthalmol J. 2012; https://doi.org/10.2174/1874364101206010054

35. Pandit J, Sultana Y, Aqil M. Chitosan-coated PLGA nanoparticles of bevacizumab as novel drug delivery to target retina: optimization, characterization, and in vitro toxicity evaluation. Art Cells Nanomed Biothechnol. 2017; https://doi.org/10.1080/21691401.2016.1243545

36. Battaglia L, Gallarate M, Peira E, Chirio D, Solazzi I, Giordano SMA, Gigliotti CL, Riganti C, Dianzani C. Bevacizumab loaded solid lipid nanoparticles prepared by the coacervation technique: preliminary in vitro studies. Nanotechnology. 2015; https://doi.org/10.1088/0957-4484/26/25/255102

37. Xie B, Jin L, Luo Z, Yu J, Shi S, Zhang Z, Shen M, Chen H, Li X, Song Z. An injectable thermosensitive polymeric hydrogel for sustained release of Avastin® to treat posterior segment disease. Int J Pharm. 2015; https://doi.org/10.1016/j.ijpharm.2015.05.071

38. De Cogan F, Hill LJ, Lynch A, Morgan-Warren PJ, Lechner J, Berwick MR, Peacock AFA, Chen M, Scott RAH, Xu H, Logan A. Topical delivery of anti-VEGF drugs to the ocular posterior segment using cell-penetrating peptides. Invest Ophthalmol Vis Sci. 2017; https://doi.org/10.1167/iovs.16-20072

39. Ambati J, Canakis CS, Miller JW, Gragoudas ES, Edwards A, Weissgold DJ, Kim I, Delori FC, Adamis AP. Diffusion of high molecular weight compounds through sclera. Invest Ophthalmol Vis Sci. 2000;41:1181-5.

40. Ambati J, Gragoudas ES, Miller JW, You TT, Miyamoto K, Delori FC, Adamis AP. Transscleral delivery of bioactive protein to the choroid and retina. Invest Ophthalmol Vis Sci. 2000;41:1186-91.

41. Maurice DM, Mishima S. Ocular pharmacokinetics. In: Sears ML, editor. Pharmacology of the Eye. Berlin: Springer-Verlag; 1984. pp. 19-116.

42. Del Amo EM, Urtti A. Rabbit as an animal model for intravitreal pharmacokinetics: Clinical predictability and quality of the published data. Exp Eye Res. 2015; https://doi.org/10.1016/j.exer.2015.05.003

Figure Captions

Fig. 1

Freeze-dried matrix used in release studies. Photo of the matrices used in both in vitro and in vivo experiments; they had sizes of 11.5 x 2.9 mm in length and diameter, respectively

Fig. 2

Release profile of FITC-dextran from matrices under study. The graph illustrates the cumulative amount released from the matrices based on plyvinylpyrrolidone (PVP-3), polyvinylalcohol (PVA-3) and hydroxypropylmethylcellulose (HPMC-3). FITC-dextran (FITC-DX) powder was used as control. (n = 3)

Fig. 3

Release profile of bevacizumab from matrices under study**.** The graph illustrates the cumulative amount released from the matrices based on polyvinylalcohol (PVA-3) and hydroxypropylmethylcellulose (HPMC-3). Bevacizumab commercial solution (BVZsol) was used as control. (n = 3)

Fig. 4

In vivo bevacizumab release. The graph illustrates the drug concentration in aqueous (AH) and vitreous humour (VH) following subconjunctival (SC) or intravitreal (IVT) administration of 0.625 mg of bevacizumab in HPMC-3 matrices (n = 6). *Statistically different from SC aqueous humour at the same time; § Statistically different from IVT aqueous humour at the same time; # Statistically different from SC vitreous humour at the same time

Fig. 5

Photos of treated eyes of rabbit. The pictures show examples of eyes at 1 and 7 days following subconjunctival (SC) or intravitreal (IVT) administration of HPMC-3 matrices loaded with bevacizumab

Fig. 6

Intraocular pressure course after surgical treatment. IOP values measured during clinical observation following subconjunctival (SC) or intravitreal (IVT) administration of HPMC-3 matrices loaded with bevacizumab. The values are reported as difference between treated and fellow eye (n = 6)

Fig. 7

Photomicrographs of retinal structure. Comparison between the retinal structures of an eye following intravitreal administration of HPMC-3 matrix loaded with bevacizumab and the untreated fellow eye. *Scale bar:* 100 μm

Figure1

Click here to download Figure Fig 1.tiff

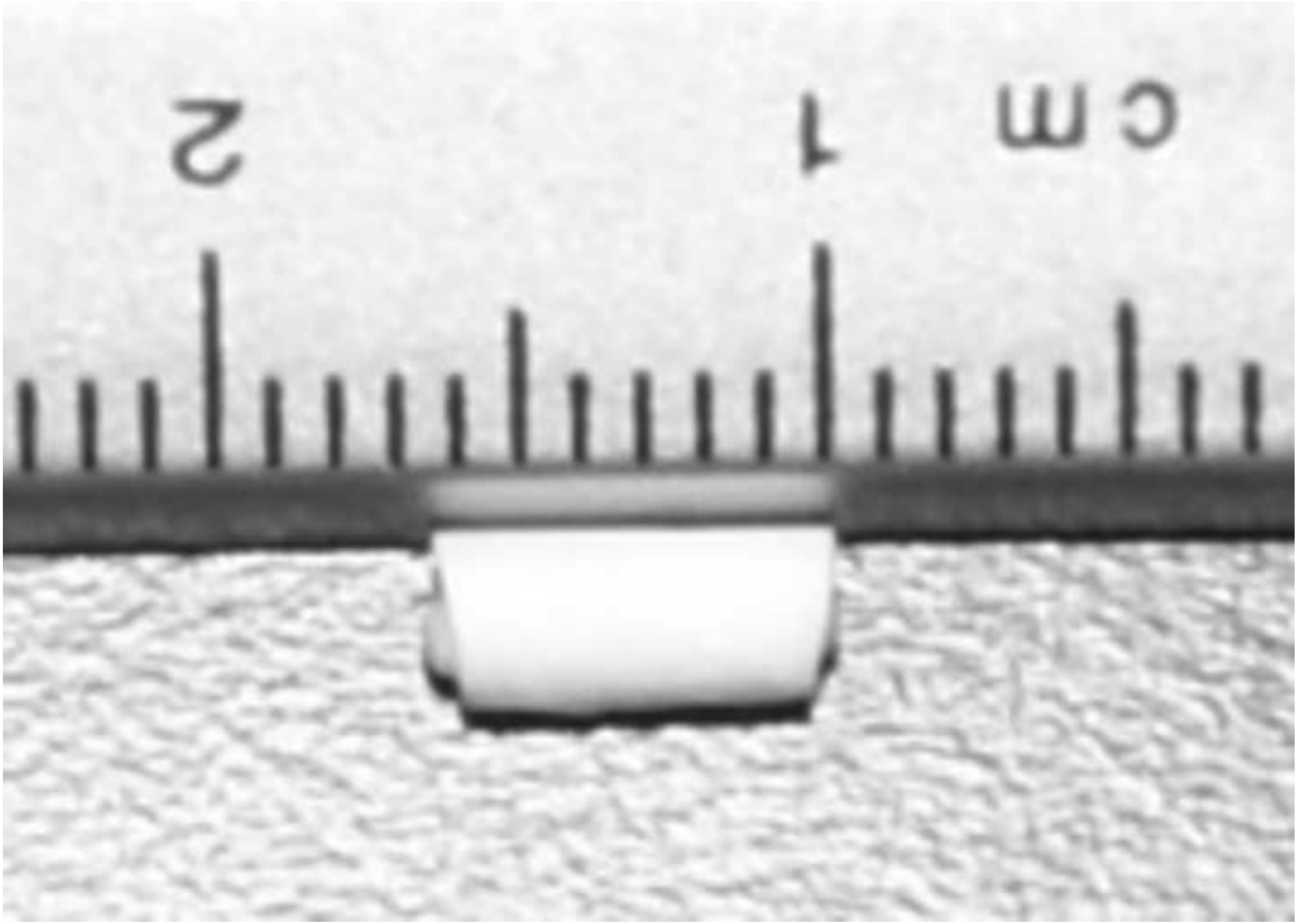

Figure2

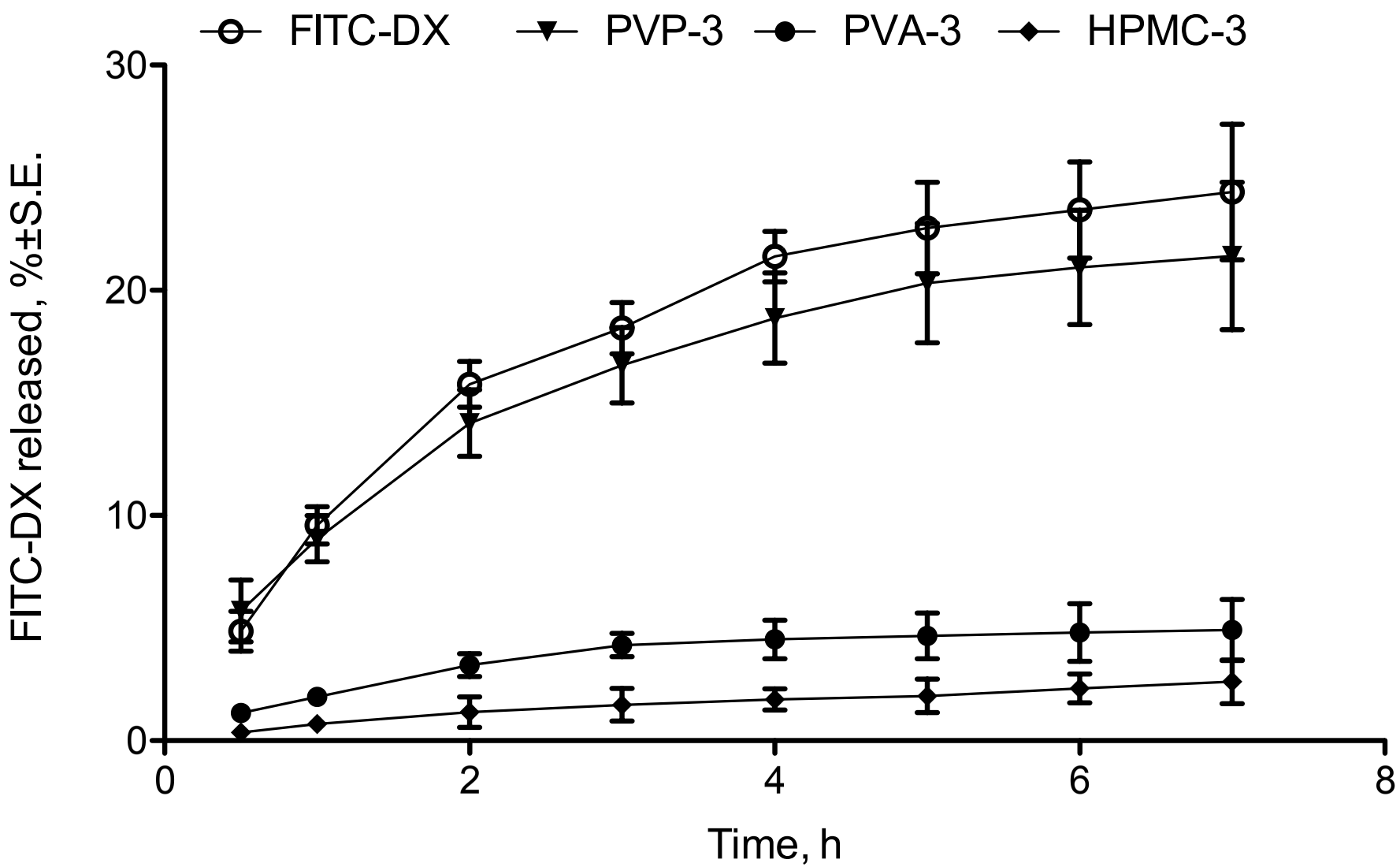
FITC-DX
PVP-3
PVA-3
HPMC-3
FITC-DX released, %±S.E.
30
20
10
0
0
2
4
6
8
Time, h

Figure3

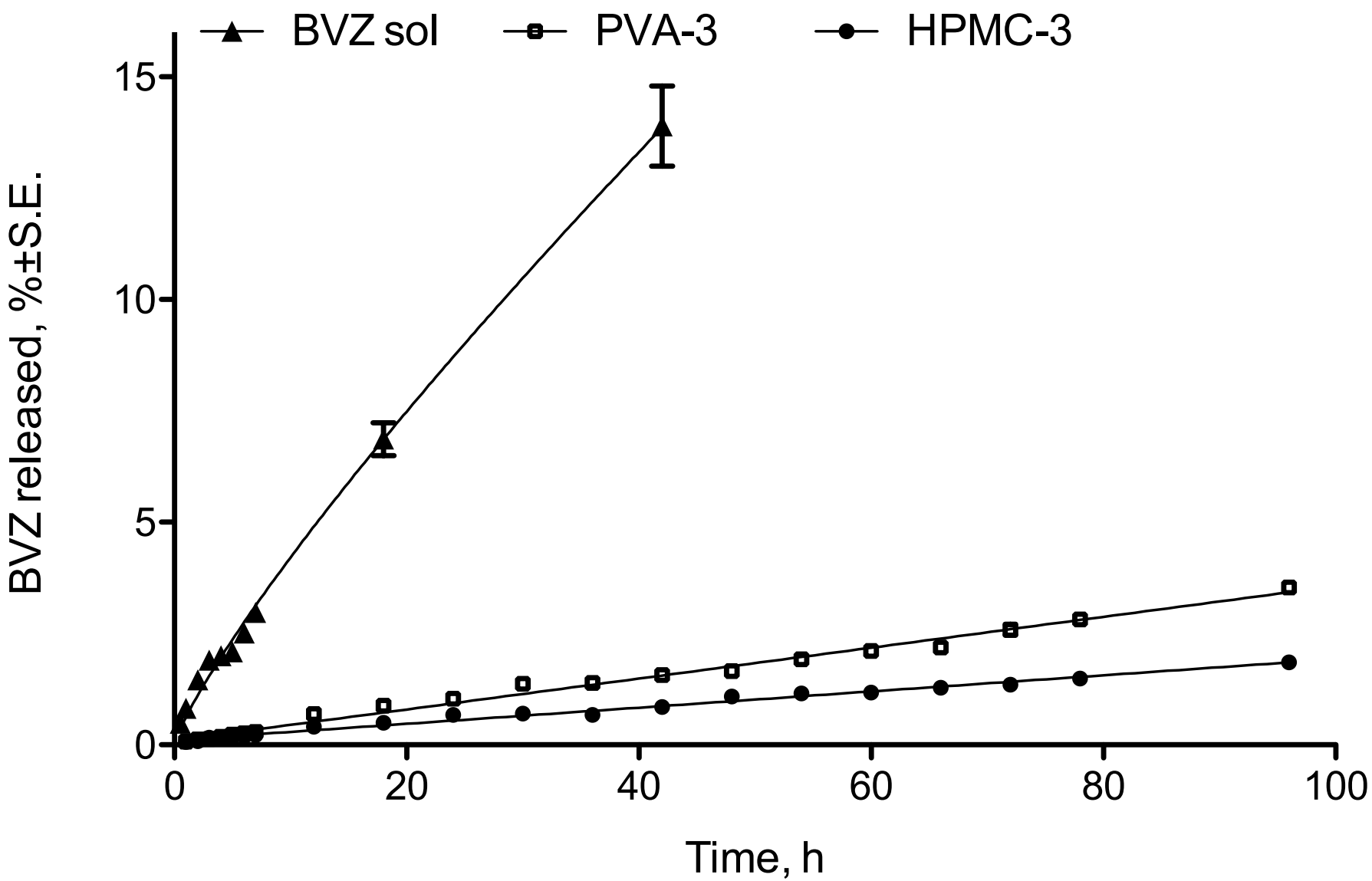
BVZ sol
PVA-3
HPMC-3
BVZ released, %±S.E.
15
10
5
0
0
20
40
60
80
100
Time, h

Figure4

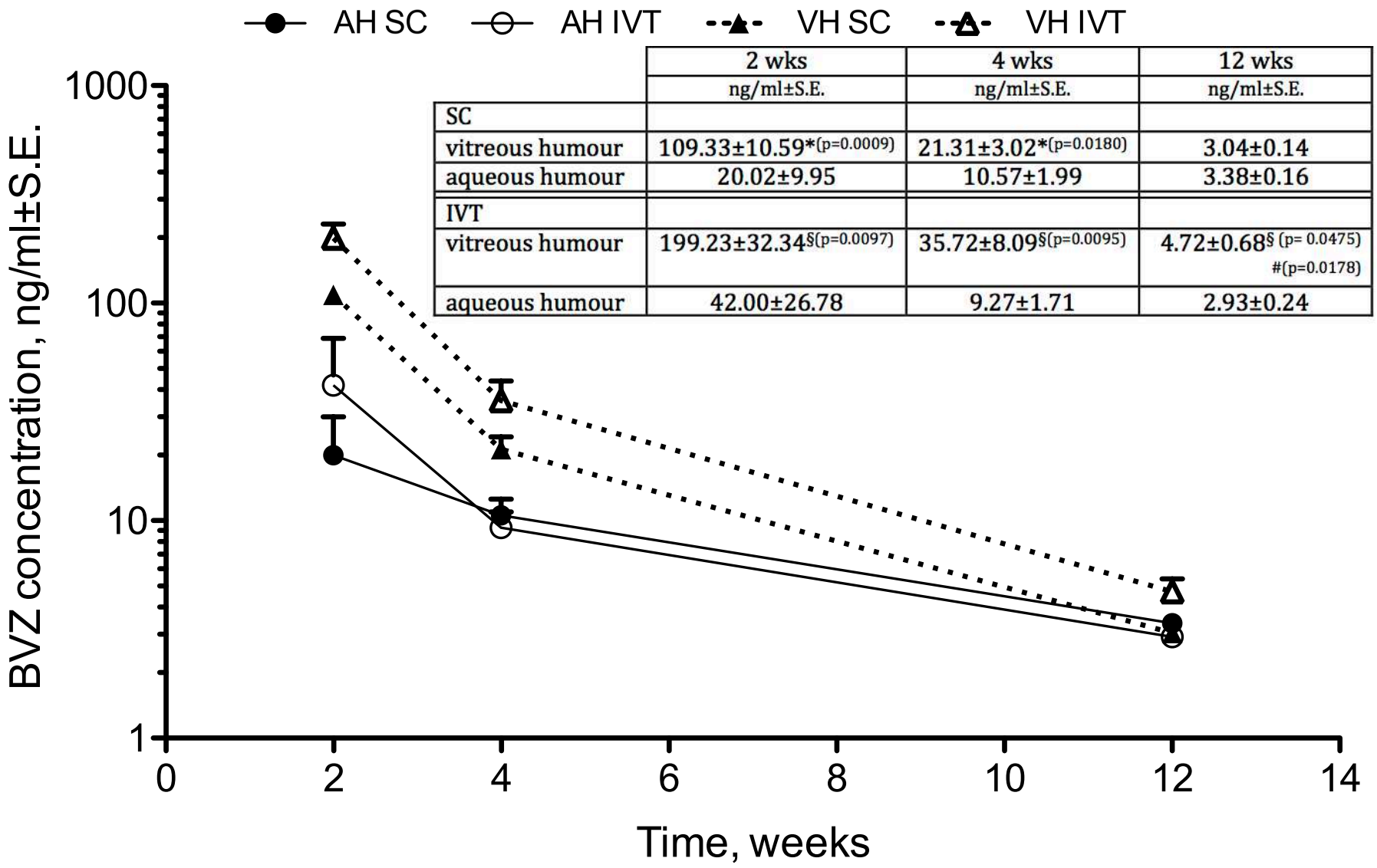

	2 wks ng/ml±S.E.	4 wks ng/ml±S.E.	12 wks ng/ml±S.E.
SC			
vitreous humour	109.33±10.59*(p=0.0009)	21.31±3.02*(p=0.0180)	3.04±0.14
aqueous humour	20.02±9.95	10.57±1.99	3.38±0.16
IVT			
vitreous humour	199.23±32.34§(p=0.0097)	35.72±8.09§(p=0.0095)	4.72±0.68§ (p= 0.0475) #(p=0.0178)
aqueous humour	42.00±26.78	9.27±1.71	2.93±0.24

Figure5

Click here to download Figure Fig 5.tiff

Figure6

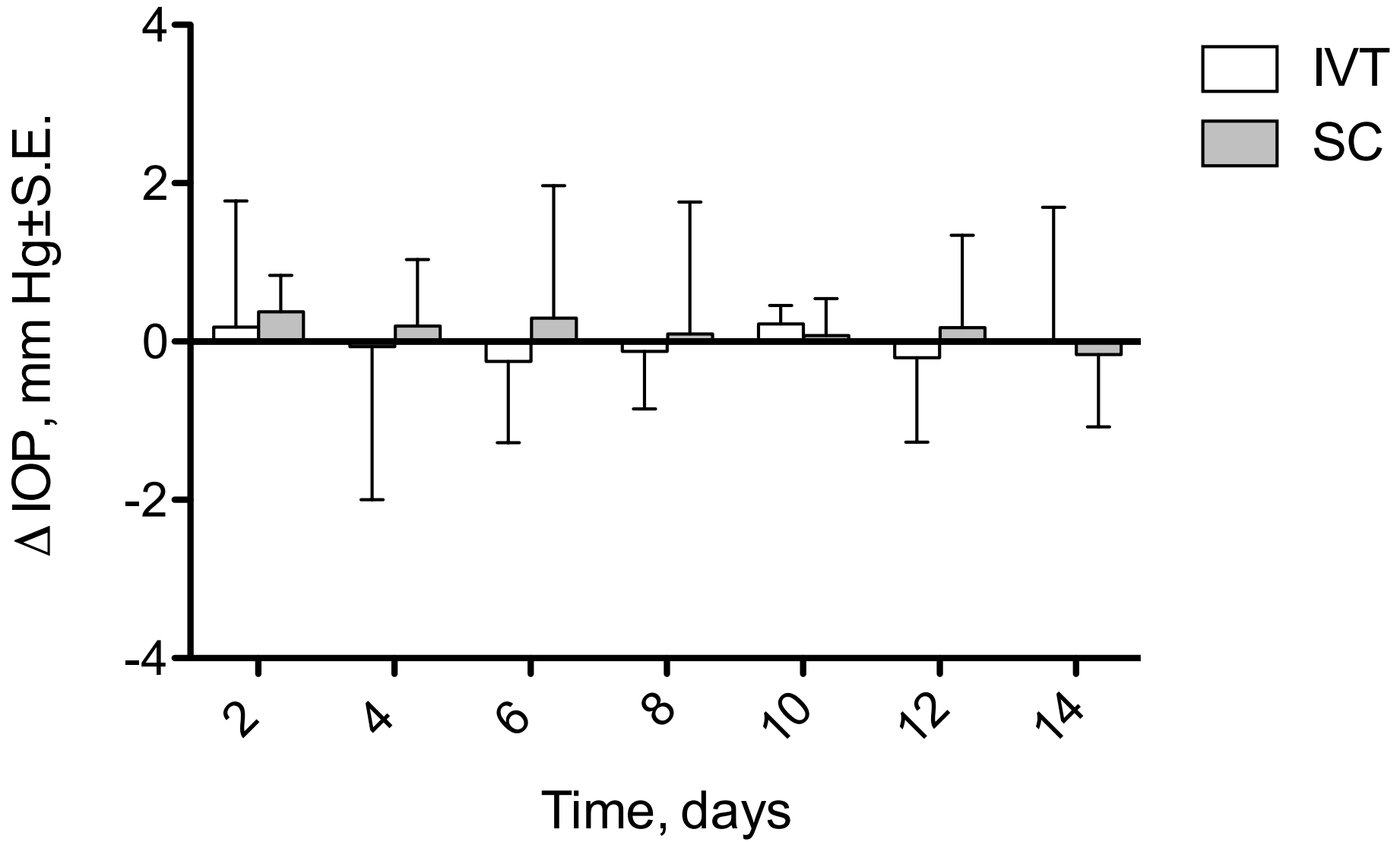

Figure7

Click here to download Figure Fig 7.tiff

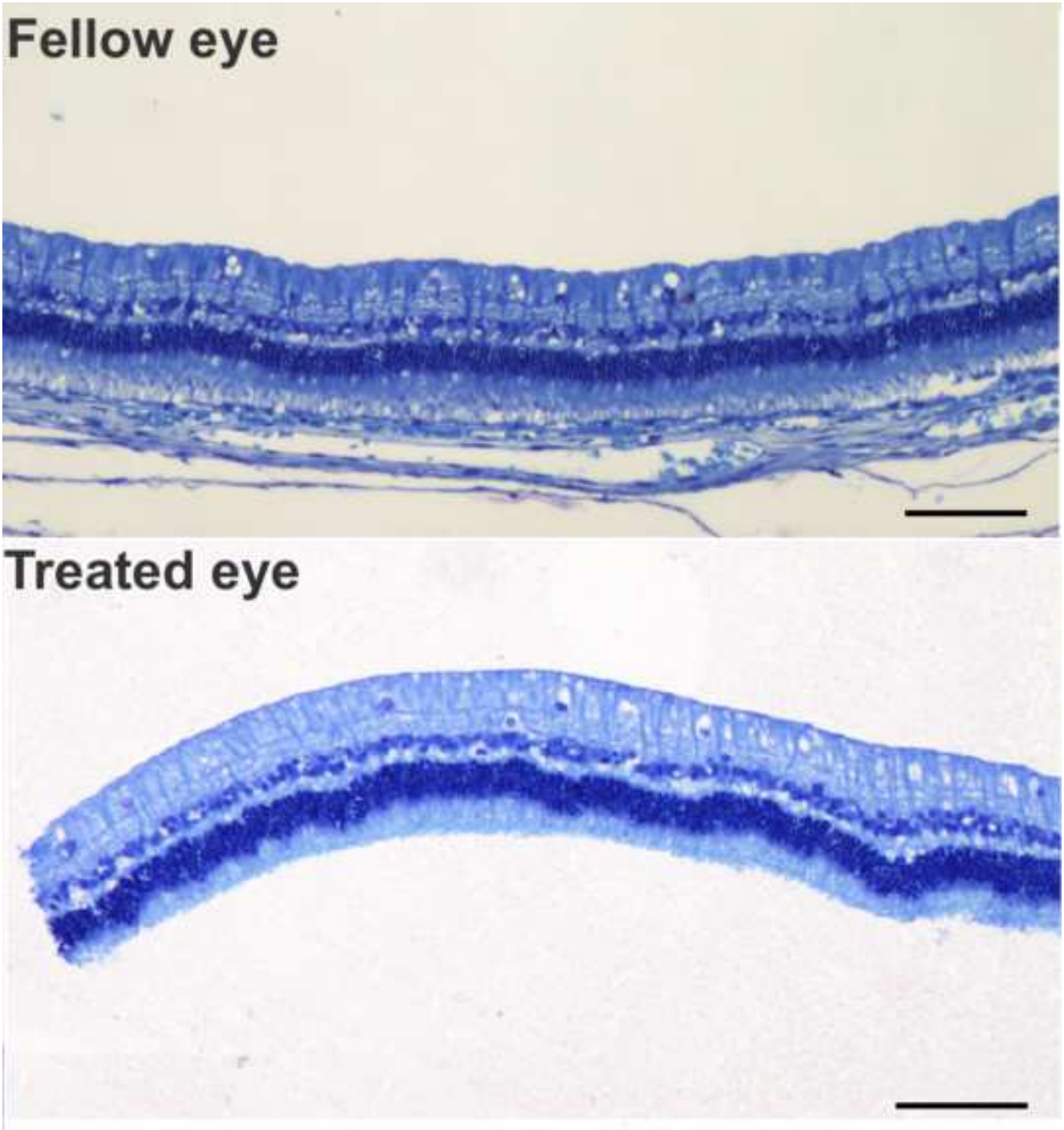

TABLE 1. Composition (% w/w) of the dispersions freeze-dried

Formulation	HPMC	PVP	PVA	PAA	Mannitol	Trehalose	Lactose	Solvent
HPMC-1	1.0	-	-	-	2.0	1.0	-	PBS[a]
PVP-1	-	3.0	-	-	2.0	1.0	-	PBS
PVA-1	-	-	3.0	-	2.0	1.0	-	PBS
PAA-2/0.3	-	-	-	0.3	2.0	1.0	-	W[b]
HPMC-2	1.0	-	-	-	2.0	1.0	-	W
PVP-2	-	3.0	-	-	2.0	1.0	-	W
PVA-2	-	-	3.0	-	2.0	1.0	-	W
PAA-2	-	-	-	0.2	2.0	1.0	-	W
HPMC-3	1.0	-	-	-	-	1.0	-	W
PVP-3	-	3.0	-	-	-	1.0	-	W
PVA-3	-	-	3.0	-	-	1.0	-	W
PAA-2.1	-	-	-	0.2	5.0	1.0	2.0	W

[a] pH 7.4 Sørensen phosphate buffer solution

[b] MilliQ water

TABLE 2. Viscosity values of the polymeric dispersions under study before and after freeze-drying and sterilization processes.

Formulation	Viscosity (mPa s)		
	Before	After freeze-drying	After sterilization
HPMC-1	411.6 (PS[a])	244.20 (PS)	41.32 (N[b])
HPMC-2	381.49 (PS)	232.81 (PS)	43.42 (N)
HPMC-3	379.10 (PS)	230.68 (PS)	46.12 (N)
PVP-1	4.36 (N)	4.98 (N)	5.17 (N)
PVP-2	24.42 (N)	25.29 (N)	24.98 (N)
PVP-3	20.62 (N)	22.38 (N)	17.68 (N)
PVA-1	2.81 (N)	2.98 (N)	2.79 (N)
PVA-2	2.78 (N)	2.53 (N)	2.16 (N)
PVA-3	2.83 (N)	2.61 (N)	2.93 (N)
PAA-2/0.3	13210 (PS)	7058 (PS)	-
PAA-2	8391 (PS)	3576 (PS)	2.86 (PS)
PAA-2.1	9674 (PS)	3256 (PS)	1.97 (PS)

[a] Pseudoplastic behaviour

[b] Newtonian behaviour

TABLE 3. Water sorption time of the matrices under study before and after the sterilization process.

Matrix	WST	
	Before	After sterilization
HPMC-1	9 min	28 min
HPMC-2	24 min	22.5 min
HPMC-3	41 min	46 min
PVP-1	4 min	18 min
PVP-2	4.5 min	4.5 min
PVP-3	11 min	11.5 min
PVA-1	60 s	5.5 min
PVA-2	100 s	90 s
PVA-3	11 min	8 min
PAA-2	5 s	2 min
PAA-2.1	immediate	immediate